Boundary Element Modelling of Printing and Coating Nips in a Sliding Contact

M.F.J. Bohan, T.C. Claypole and D.T. Gethin

Keywords: boundary element modelling, inkflow

Abstract

Printing and coating nip contacts are one of the most generic and difficult areas to model successfully. A boundary element numerical model is described, which has been applied to a sliding nip contact. It models the interaction between the soft elastomer covering on the roller and the coating / printing fluid. This is a continuation of earlier work [1] and represents contacts commonly found in the printing and coating industry. A parametric investigation is used to evaluate different processes and configurations. The results highlight the main roller train design and operating parameters for ink transfer in nip contacts. An orthogonal array technique has been successfully applied to the numerical simulation of the nip contact to optimise the output from the model.

Introduction

The transfer of fluid to a base substrate in a controlled manner is used in many printing and coating applications. This is effected by the use of alternate solid and rubber-coated rollers in contact, Figure 1. These may operate in either a rolling or a sliding configuration dependent on the application, with some lateral sliding in certain instances. There is a pressure or engagement applied between

the two rolls which for low levels can produce large deformations in the rubber roller surface.

As the fluid flows through the nip contact pressure is generated. This pressure field will lead to the deformation of the elastomeric layer and this deformation will affect the film thickness and hence the pressure in the nip contact. This contact is referred to as that of Soft Elasto Hydrodynamic Lubrication (Soft EHL) in a line contact.

Evaluation of nip contacts has been extensively reported in the literature both experimentally and numerically. One of the initial studies [2] evaluated a dry contact and this provided the basis for much of the subsequent analysis. This provided an integral expression for the contact pressure and additional parameters. This has been further developed [3] for an infinite plane layer, parameters investigated include the Poisson's ratio and layer thickness which affected the geometry of the roller surface and the size of the contact width. This has been further developed providing an understanding of dry / severely starved contacts [4], [5].

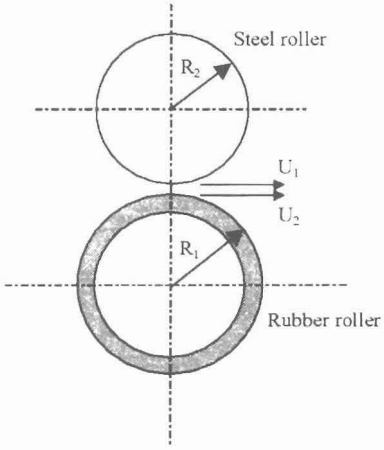

Figure 1 Schematic representation of a nip contact

The analysis of a wet contacts has been considered, one of the first [6] evaluating this on a hard roller pair rotating against a soft polythene target. An inlet / outlet zone analysis [7] was used to evaluate large deformations in the contact. This assumed a Hertzian profiles in the centre of the contact. This was further simplified [8] by analysis of the inlet zone and a Hertzian contact, as it had been shown that the outlet nip zone has little impact on the nip performance.

The iterative strategy between the fluid film and elastomeric surface for the solution of the soft EHL problem was highlighted in [9]. This has been extended

[10] to examine different regimes of lubrication dependent on the inlet nip condition. Applications in printing have been applied only recently [11], which evaluated the case of flooded and starved nips. Further work has evaluated rolling in the contact using both finite [12] and boundary element [13] techniques.

This paper focuses on the numerical evaluation of a nip contact in rolling and sliding, as found in typical ink roller trains, fount supply systems and multi roll coating applications. The problem is solved using boundary element techniques, with the fluid in the nip contact assessed being Newtonian in nature, though this can be expanded to non-Newtonian at a later date, which may be more appropriate to certain applications.

Orthogonal array techniques

The study evaluating the effects of various parameters on the pressures and flow rates was carried out using orthogonal array methods [14]. These allow multiple parameters to be evaluated simultaneously along with possible interactions. These have been successfully used in an experimental analysis of printing press performance [15]. Traditional experimental methods such as full factorial and elimination have several disadvantages including the number of experiments, time required, not covering the full range of combinations and the repeatability.

The orthogonal arrays provide a balanced sub set of the full factorial allowing all parameters to be properly investigated. It is possible to analyse a number of different parameters simultaneously, in a minimum of experiments. The arrays used were L_{16} which were utilised such that they analysed for eight parameters at two levels with any possible interactions between the sliding velocity and the other parameters investigated. The linear graph for the array is shown in Figure 2, with parameter 1 being the effect of roller sliding. Orthogonal array techniques have been extensively applied to experimental situations but its application to numerical studies relatively new and innovative.

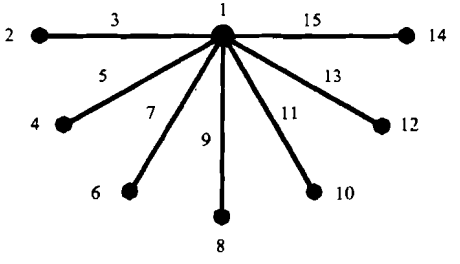

Figure 2 Linear graph for L_{16} array

Model background theory

The solution of the elastohydrodynamic lubrication problem encountered in printing and coating applications requires the solution of both the elastic deformation of the rubber roller and that of the Reynolds equation. These two solutions need to be linked resulting in an iterative solution process. The background theory to the solution of each will be discussed followed by their coupling and the solution technique.

Elastic deformation

Assuming the rubber layer on the roller to be linearly elastic, for a plain strain case, the boundary element integral equation for the solution of the general problem of elastostatics is given below

$$c_{lk}^{i}u_{k}^{i}+\int_{\Gamma}p_{lk}^{*}u_{k}d\Gamma=\int_{\Gamma}u_{lk}^{*}p_{k}d\Gamma+\int_{\Omega}u_{lk}^{*}b_{k}d\Omega \qquad \ldots 1$$

However, for the problem examined, the body forces are zero with no thermal or gravitational forces and the equation can be simplified to

$$c_{lk}^{i}u_{k}^{i}+\int_{\Gamma}p_{lk}^{*}u_{k}d\Gamma=\int_{\Gamma}u_{lk}^{*}p_{k}d\Gamma \qquad \ldots 2$$

Reynolds equation

The Reynolds equation provides the governing equation for a Newtonian fluid flow. If the contact width is small in comparison with the roller diameter and the analysis plane is some distance from the roller edge

$$\frac{d}{dx}\left[\frac{h^{3}}{12\mu}\frac{dp}{dx}\right]=\left(\frac{u_{1}+u_{2}}{2}\right)\frac{dh}{dx} \qquad \ldots 3$$

The assumption of a Newtonian fluid has been made in much of the published data [11], [16], although some printing inks are non-Newtonian and this can affect the flow characteristics [17]. The Swift-Steiber boundary conditions were applied, with the pressure at the inlet and outlet equalling zero and the pressure gradient at the outlet being zero. This was set automatically within the code and effectively sets the rupture point in the contact to ensure flow continuity.

This equation was solved using Green's function with the right hand side of equation (3) replaced by the Dirac delta function $\delta(x-\zeta)$. The solution can be obtained using the following for $g(x,\zeta)$ and its differential, where $h^* = h^3$.

$$g(x,\zeta)=\begin{cases}\int_{\zeta}^{x}\frac{1}{2h^*}dx\ for\zeta>x\\ -\int_{\zeta}^{x}\frac{1}{2h^*}dx\ for\zeta<x\end{cases},\quad \frac{dg(x,\zeta)}{dx}=\begin{cases}\frac{1}{2h^*} & for\quad \zeta>x\\ -\frac{1}{2h^*} & for\quad \zeta<x\end{cases} \qquad \ldots 4$$

Using equation (4) and the Dirac function, the Reynolds equation (3) can be solved providing the following expression for the pressure

$$p(\zeta)=\left[-h^*(x_1)g(x_1,\zeta),h^*(x_2)g(x_2,\zeta)\right]\begin{bmatrix}v_1\\ v_2\end{bmatrix}+$$
$$\left[h^*(x_1)\frac{dg}{dx}\Big|_{x=x_1},-h^*(x_2)\frac{dg}{dx}\Big|_{x=x_2}\right]\begin{bmatrix}p_1\\ p_2\end{bmatrix}+\int_{x_1}^{x_2}\psi(x)\cdot g(x,\zeta)dx \qquad \ldots 5$$

Film thickness

The film thickness was defined using the following equation using equivalent roller radius. A negative value of h_0 indicates a roller engagement.

$$h(x)=h_0+\frac{x^2}{2R}+u(x) \qquad \ldots 6$$

Load

Closure of the solution is obtained by the load meeting the following criteria

$$\int_{x_1}^{x_2} p.dx = L \qquad \ldots 7$$

Solution of the equations

The solution utilises linear elements in a finite plane model, which allows the analytical evaluation of the element integrals. The boundary of the elastomer is

divided into a number of elements, Figure 1, to obtain the integrals in the elasticity equation (6). Each of these integrals can be represented by the sum of integrals on the boundary elements.

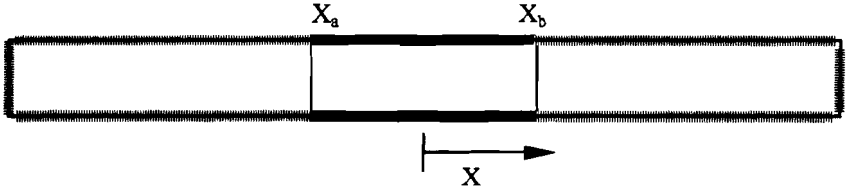

Figure 3 Schematic discretization of boundary layer

Numerical singularities can occur when a field point ζ_0 is located at a node where the integration takes place. These can be eliminated with the use of corner factors and the techniques are indicated in [18], [19].

The following represents the solution procedure

1. Set an initial value for the engagement, h_0, from this the Hertzian pressure and the consequent indentation is calculated.
2. The film thickness is calculated in the nip junction.
3. The film pressure is calculated.
4. The indentation is recalculated.
5. If the indentation has not met the convergence criterion, then repeat from stage (2) with the new indentation.
6. Once the indentation criterion has been meet, examine the load equilibrium. If this is not met then appoint a new value for h_0 and repeat from (1).

Results and discussion

The case studies illustrate examples of situations found in both printing and coating applications, with the results being applicable to other soft EHL nip contacts in siding. The results are divided into two sections. The first represents a systematic evaluation into the effect of sliding and the second the application of orthogonal array techniques perform numerical experiments to establish the influence of each of the process parameters and the possible interactions.

The convergence requirement for the analysis was 0.1 percent on the pressure and indentation. Convergence of the solutions was obtained in approximately 500 iterations.

The effect of sliding on a roller nip contact

The process parameters used in the evaluation of the impact of roller sliding on the film pressure, film thickness and flow rate are given in Table 1. Two case studies were investigated representing typical applications found in offset printing presses and in multi-roll coaters. These parameter values were held constant while the relative slip between the two rollers was altered.

Application	Load	Roller speed	Viscosity	Roller radius	Elastic modulus	Rubber thickness
Printing	1500 Nm^{-1}	2.0 ms^{-1}	4 Pa.s	0.050 m	2.0e+6 2.0e+11	8 mm
Coating	3000 Nm^{-1}	2.25 ms^{-1}	1 Pa.s	0.125 m	2.0e+6 2.0e+11	14 mm

Table 1 Process parameters used for sensitivity study

The effect of roller sliding on a printing application is shown in Figure 4. The rolling solution represents roller surface speeds of 2.0 ms^{-1}, with the speed of roller 1 altered between 1.5 ms^{-1} and 2.5 ms^{-1}. The sliding clearly does not alter the pressure profile in either its maximum value or the contact width. There is only a small change in the film thickness with a reduction in the minimum value, as the speed of roller 1 reduces. These figures also display the nip contact width derived from the analysis.

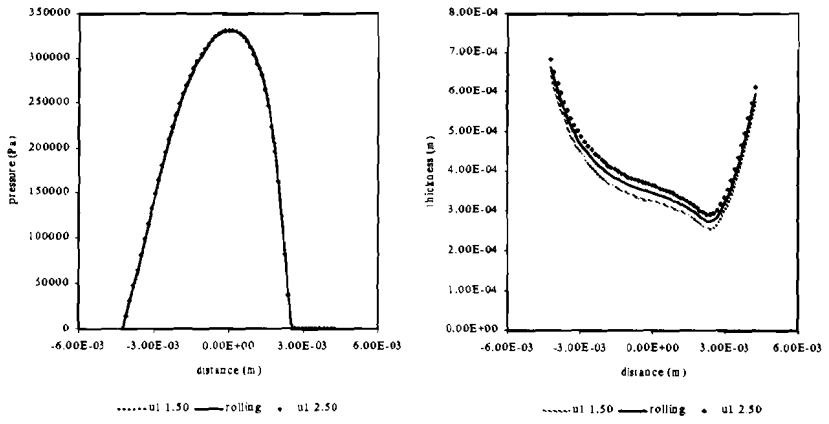

Figure 4 Pressure and film thickness variations for different sliding speeds (u_1 = 1.5-2.5 ms^{-1}, u_2 = 2.0 ms^{-1})

The velocity profiles for a Newtonian fluid through the nip can be defined using the following equation (8). The u_1 and u_2 terms represent the contribution due to the Couette flow from each roller, with the pressure gradient, $\frac{dp}{dx}$, also affecting the flow. This assumes a no slip condition between the fluid and roller surface.

$$u(y) = u_1\left[1 - \frac{y}{h}\right] + u_2\left[\frac{y}{h}\right] - \frac{dp}{dx}\frac{1}{2\mu}\left[hy - y^2\right] \quad \ldots 8$$

Velocity contours for a pure rolling contact are presented, Figure 5. These show symmetry about the centre of the fluid film with an increase in velocity through the nip. The velocity of the film at the inlet is much lower resulting in high levels of shear in the fluid, most significant near the surface of the roller. This is in agreement with earlier work [11], [17]. The shear rates reduce in the centre of the contact with shear increasing at the outlet near the rupture point. The outlet velocity is much larger in the centre of the contact than that of the roller surfaces, representing the pumping capacity within the nip contact.

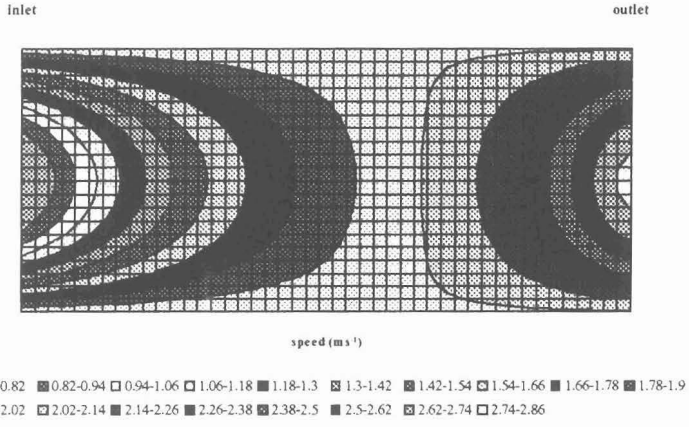

Figure 5 Velocity profile through the nip for a rolling contact (u_1 = 2.0 ms^{-1}, u_2 = 2.0 ms^{-1})

The velocity profiles for the sliding case, Figure 6, are significantly different from those of the rolling, shown in Figure 5, with a large skew in the profiles. There is a variation in velocity through the whole of the contact region. The rate of shear at the inlet is also increased with the highest levels nearest to the fastest roller surface, located at the bottom of the figure. At the outlet, the rates of shear

are greater towards the slower of the two roller surfaces. These results have implications for non-Newtonian fluids where the shear rates affect the viscosity of the fluid, which can have a major effect on the flow rate. This will be discussed in detail in the following parametric study.

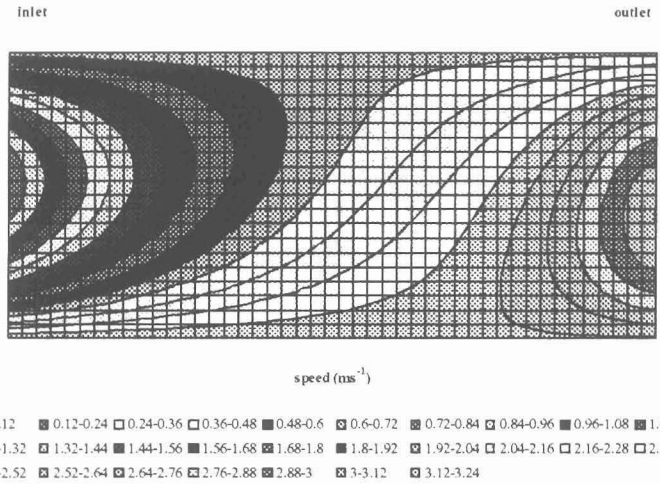

Figure 6 Velocity profile through the nip for a sliding contact (u_1 = 2.5 ms^{-1}, u_2 = 2.0 ms^{-1})

The flow rate, Q(x), can be calculated analytically using equation 9 and there is a significant change in the flow rate with the sliding between the two rollers, Figure 7.

$$Q(x) = \left(\frac{U_1 + U_2}{2} \right) h - \frac{h^3}{12\mu} \frac{dp}{dx} \quad \ldots 9$$

This flow rate is significant, with approximately a 2 percent change for only a 2.5 percent alteration in the speed of roller 1. These speed changes are apparent in printing presses [20] with rollers in normal "rolling contact". This speed differential is a consequence of micro slippage at the roller engagement. In the context of the present work, the flow rate change may occur during printing. Any changes in the roller speeds will affect the quality and consistency of the printed product. The variation in the flow rate is three times larger than the change in the minimum film thickness. This indicates the calculation of the film thickness is only a means to an end in the determination of the fluid flow in the system. The extreme points in Figure 7 show the near linear divergence of flow rate with sliding speed.

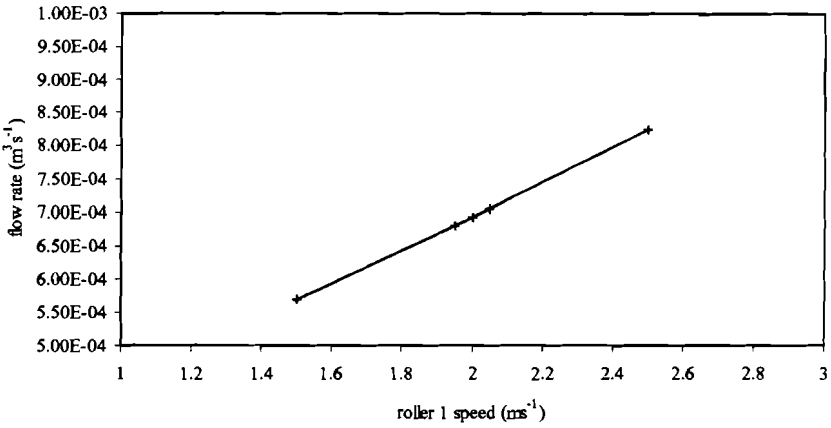

Figure 7 Change in flow rate for different sliding speeds (u_1 = 1.5-2.5 ms^{-1}, u_2 = 2.0 ms^{-1})

The results show significant variations in flow characteristics when sliding is introduced into the roller train. The flow rate is altered for small changes in the roller speed. The model may also be applied to coating applications, such as multi roll coaters, where the sliding is used as a metering tool for the fluid flow. The pressure profiles and film thickness characteristics for the case stated in Table 1 are shown in Figure 8. These are for a fully flooded condition and the rupture point is significantly closer to the centre of the nip than the start point. The pressure profile through the nip is again similar in all cases with a very small fluctuation in the inlet profile. As the relative sliding speed reduces from 2.25 ms^{-1} to 0.25 ms^{-1}, the film thickness also reduces though the shape remains consistent.

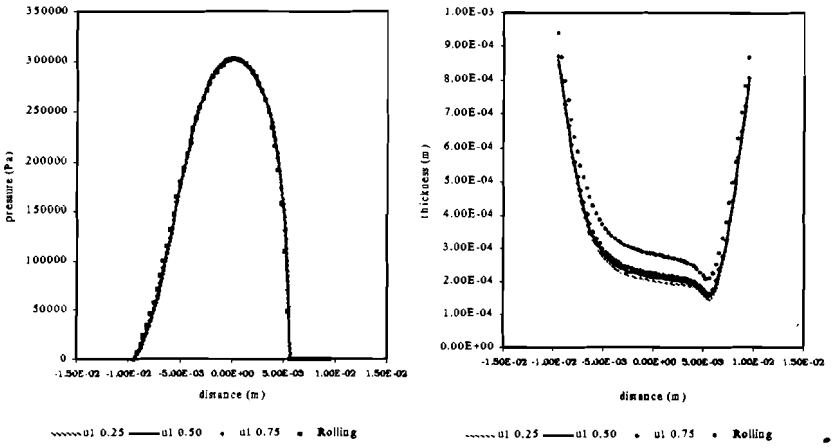

Figure 8 Pressure and film thickness variations for different sliding speeds (u_1 = 0.25, 0.50, 0.75, 2.25 ms^{-1}, u_2 = 2.25 ms^{-1})

The change in speed (u_1) affects the flow rate through the nip, Figure 9, with a reduction in the total flow through the nip. The relationship shows a slight non-linearity as the speed of roller 1 is reduced. The results show that even with a zero velocity with one of the rollers there can still be a significant flow through the nip contact.

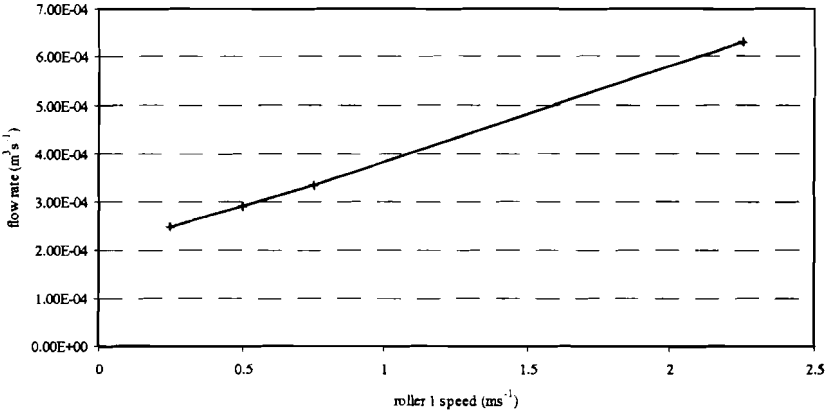

Figure 9 Change in flow rate for different sliding speeds (u_1 = 0.25-2.25 ms^{-1}, u_2 = 2.0 ms^{-1})

The high relative sliding between the two roller surfaces generated much higher velocity gradients, Figure 10. Because of the reduced entrainment by the rollers, there is now some flow reversal from within the nip near to the roller with the lower surface speed. This is reflected by the recirculating roll at the entry to the nip. Once outside this region, the velocity contours are relatively even across the nip with even rates of shear between the two roller surfaces.

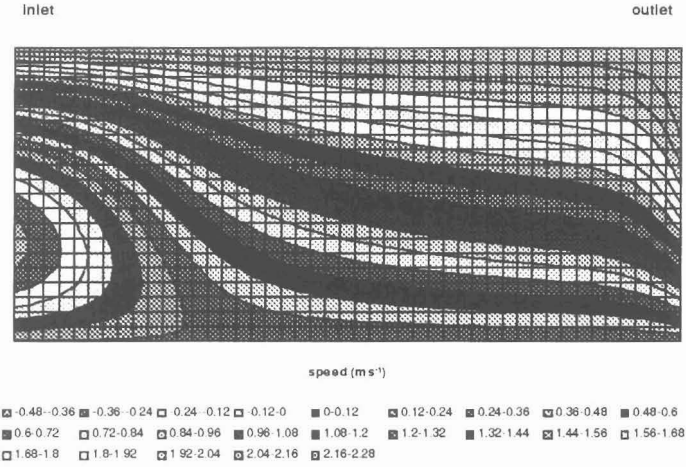

Figure 10 Velocity profile through the nip for a sliding contact (u_1 = 0.25 ms^{-1}, u_2 = 2.25 ms^{-1}, μ = 1 Pa.s)

Orthogonal array evaluation of the sensitivity of the process

Orthogonal arrays were utilised in a parametric study to evaluate the influence of various process parameters on the performance of the nip contact. An L_{16} array was used and the levels for the eight parameters investigated are shown in Table 2. The levels selected represent the range of values found in a typical roller train.

Parameter	Level 1	Level 2
Sliding speed	+0%	+5%
Load	1500 Nm^{-1}	1750 Nm^{-1}
Roller speed	2.0 ms^{-1}	2.5 ms^{-1}
Viscosity	4 Pa.s	5 Pa.s
Roller radius	0.050 m	0.045 m
Elastic modulus	2.0e+6	1.5e+6
Rubber thickness	8 mm	12 mm

Table 2 Parameter levels used in the orthogonal array investigation

Analyses of the influence of numerous quality characteristics were carried out including the maximum pressure, minimum film thickness and flow rate. It was not possible to analyse for pressure and film thickness profiles as the contact width varied simultaneously dependent on parameter changes making addition impossible. Results for the effect for each of the parameters evaluated on the maximum pressure and contact width are shown in Figure 11. All the parameters evaluated have a similar relative effect on both the pressure and the contact width and as expected, the load has the most significant influence on both of these. After this the significant parameters are all related with the physical properties of the two rollers in the contact. There is little or no effect from the ink rheology or the speeds of the two rollers since the fluid is Newtonian in this analysis.

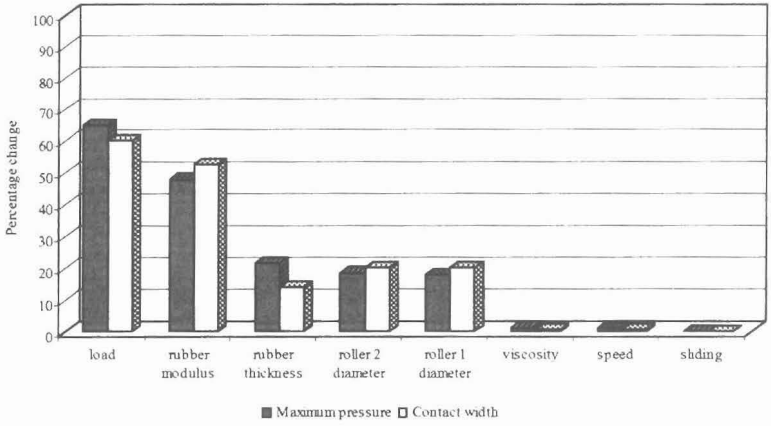

Figure 11 Variation of pressure and contact width for each parameter within the orthogonal array experimental programme

The main parameters effecting the flow rate and film thickness are the roller speed and the fluid viscosity, Figure 12. This shows the parameters that were effecting the pressure having very little effect on the flow in the nip, with the exception of the elastic modulus of the rubber. There is also a difference between the effects of flow rate and film thickness. The most significant effect on the film thickness being the ink viscosity and the roller surface speed. However, when considering the flow rate the speed is the dominant term. Although the ink film thickness is increased by increasing the ink viscosity, the pressure term in the velocity profile is reduced with the net result of a smaller change than that detected from the roller speed.

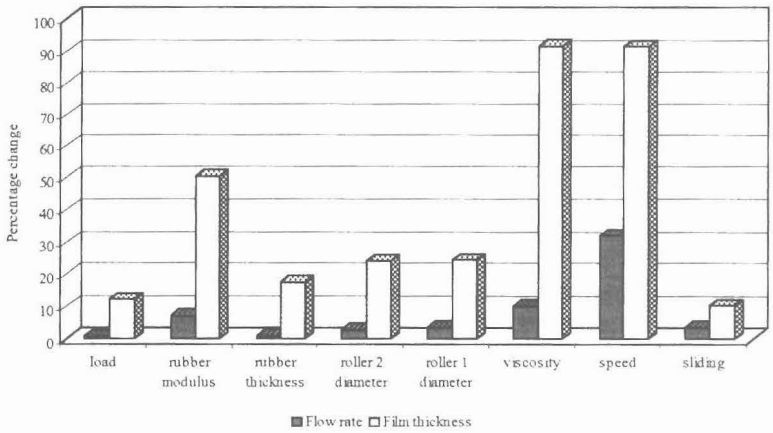

Figure 12 Variation of flow rate and film thickness for each parameter within the orthogonal array experimental programme

However, by equating all the changes to the same amount at 25% the relative effects of the different parameters become markedly different, Figure 13. The speed and sliding become the two most significant parameters, followed by the ink viscosity, roller geometry and modulus all at similar values. These results indicate that the flow will be seriously affected by speed changes, but also by the replacement (and long term use) of roller coverings within the inking train which will alter the mechanical properties of these coverings.

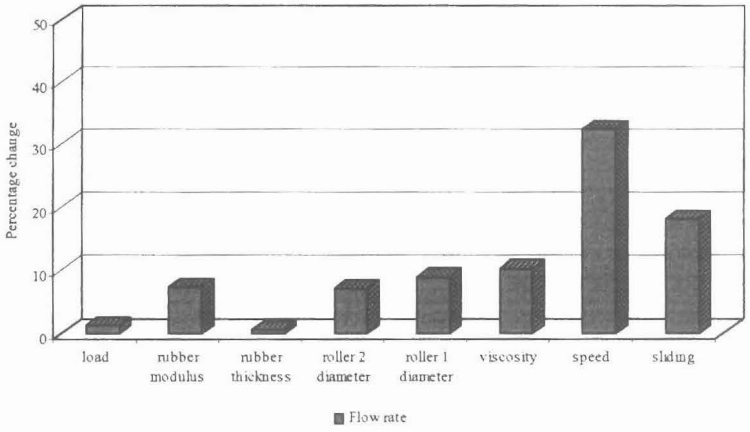

Figure 13 Variation in flow rate for equal change in all parameters

Analysis of the interactions between the roller sliding and other parameters investigated showed no significant changes in the pressure, film thickness or flow rates. This would be expected as the fluid analysed is Newtonian in nature and the viscosity is not effected by the shear rate.

Conclusions

A fast and computationally efficient boundary element model has been developed for the analysis of a sliding soft elastohydrodynamically lubricated contact for a Newtonian fluid. The numerical analysis couples the solution of the Reynolds equation and those of the elastostatics. The analysis of the sliding condition has been carried out for both micro (printing, slippage) and macro sliding (coating, fount supply). The results from this can be summarised as

- Little effect on the pressure profiles or contact widths in the contact with sliding.
- Small effect on the film thickness in the nip contact with sliding.
- Significant changes in the flow rate through the nip, even at the small sliding speeds found in printing presses.
- Higher shear rates are developed within the film.

Orthogonal array techniques have been successfully applied to assess the sensitivity of the process to parameter changes, for numerous quality characteristics. These results show

- Monitoring the load gives no indication of change in flow rate.
- The flow rate is significantly affected by the print speed, sliding between rolls, fluid viscosity, rubber modulus and. roller geometry.
- No interactions were found between the sliding speed and any of the parameters investigated.

The use of relative motion between rolls would provide a good means of control for the supply of ink in a printing train.

Acknowledgements

The authors wish to acknowledge the financial support of the European Community, Welsh Development Agency and the European Regional Development Fund.

Notation

b_k	body forces within boundary domain
c_{lk}^i	corner factor for the boundary integral equation
g	fundamental solution of Reynolds equation
h	fluid film thickness
L	load
p	fluid pressure
p_k	traction for the boundary integral equation
p_{lk}^*.	traction for Kelvin solution
p_n	fluid pressure at point x_n
R	equivalent roller radius
u_1, u_2	roller surface velocities
u	surface indentation
u_k	displacement for the boundary integral equation
u_{lk}^*	displacement for Kelvin solution
v_n	pressure gradient $\frac{dp}{dx}$ at point x_n
x	co-ordinate for film
Γ	boundary surface
δ	Dirac delta function
ζ	point on the boundary
μ	fluid viscosity
ψ	term within the Reynolds equation
Ω	boundary domain

References

1 Bohan, M.F.J., Claypole, T.C., Gethin, D.T. and Basri, S.B. "Application of boundary element modelling to printing presses", 49th Annual TAGA Tech. Conf., Quebec City, Canada, May 1997.

2 Hannah, M. "Contact stress and deformation in a thin elastic layer", Quarterly Journal of Mechanics and Applied Maths, 4, p 94-105, 1951.

3 Miller, R.D.W. "Some effects of compressibility on the indentation of a thin elastic layer by a smooth rigid cylinder", Applied Scientific Research, 16, p 405-424, 1966.

4 Meijer, P., "The contact problem of a rigid cylinder on an elastic layer", Applied Scientific Research, 18, p 353-383, 1968.

5 Jaffar, M.J. "Determination of surface deformation of a bonded elastic layer indented by a rigid cylinder using Chebyshev series method" Wear, 170, p 291-294, 1993.

6 Bennett, J. and Higginson, G.R., "Hydrodynamic lubrication of soft solids", Proc. I.Mech.E. Journal of Mechanical Engineering Sciences, 12, p 218-222, 1970.

7 Hooke, C.J. and O'Donoghue, J.P., "Elastohydrodynamic lubrication of soft, highly deformed contacts", Proc. I.Mech.E., Journal of Mechanical Engineering Sciences, 14, p 34-48, 1972.

8 Gupta, P.K., "On the heavily loaded elastohydrodynamic contacts of layered solids", Trans. ASME, J. Lubric. Tech., 98, p 367-374, 1976.

9 Cudworth, C.J. "Finite element solution of the elastohydrodynamic lubrication of a compliant surface in pure sliding", 5th Leeds-Lyon Symp. on Tribology, Leeds, 1979.

10 Hooke, C.J. "The elastohydrodynamic lubrication of a cylinder on a elastomeric layer", Wear, Vol. 111, 1986.

11 MacPhee, J., Shieh, J. and Hamrock, B.J., "The Application of Elastohydrodynamic Lubrication Theory to the Prediction of Conditions Existing in Lithographic Printing Press Roller Nips"; Advances in Printing Science and Technology, 21, p 242-276, 1992.

12 Bohan, M.F.J., Lim, C.H., Korochkina, T.V., Claypole, T.C., Gethin, D.T. and Roylance, B.J. "An investigation of the hydrodynamic and mechanical behaviour of a soft nip in rolling contact", Accepted by the IMechE, 1997.

13 M.F.J. Bohan, T.C. Claypole, D.T. Gethin and S.B. Basri "Application of boundary element modelling to printing presses", 49th Annual TAGA Tech. Conf., Quebec City, Canada, May 1997.

14 Phadke, M.S., "Quality engineering using robust design", 1989 (Prentice Hall Int).

15 Bohan, M.F.J., Claypole, T.C. and Gethin, D.T. "Factors affecting the process stability of a heat set web offset press", 1st TAGA/IARIGAI Tech. Conf., Paris, France, September 1995.

16 Bohan, M.F.J., Lim, C.H., Korochkina, T.V., Claypole, T.C., Gethin, D.T. and Roylance, B.J. "An investigation of the hydrodynamic and mechanical behaviour of a soft nip in rolling contact", Proc. IMechE part J Engineering Tribology, vol. 211 no. J1, pp37-50, 1997.

17 Lim, C.H., Bohan, M.F.J., Claypole, T.C., Gethin, D.T. and Roylance, B.J. "A finite element investigation into a soft rolling contact supplied by a non-newtonian ink", J. Phys. D: Appl. Phys, vol. 29, pp 1894-1903, 1996.

18 Brebbia, C.A. and Dominguez, J. "Boundary elements: An introductory course", McGraw Hill, 1989.

19 Banerjee, P.K. and Butterfield, R. "Boundary element method in engineering science", McGraw Hill, New York, 1981.

20 Lim, C.H. "An elastohydrodynamic behaviour of a soft printing roller nip", PhD thesis, U.W. Swansea, 1995.